World Electric Vehicle Journal

MDPI

Article

Parameter Matching Method of a Battery-Supercapacitor Hybrid Energy Storage System for Electric Vehicles

Fengchen Liu, Chun Wang * and Yunrong Luo

School of Mechanical Engineering, Sichuan University of Science and Engineering, No.519, Huixing Road, Zigong 643000, China; suseLiufengchen@outlook.com (F.L.); yunrong_luo@suse.edu.cn (Y.L.)
* Correspondence: wangchun@suse.edu.cn

Abstract: To satisfy the high-rate power demand fluctuations in the complicated driving cycle, electric vehicle (EV) energy storage systems should have both high power density and high energy density. In order to obtain better energy and power performances, a combination of battery and supercapacitor are utilized in this work to form a semi-active hybrid energy storage system (HESS). A parameter matching method of battery-supercapacitor HESS for electric vehicles (EVs) is proposed. This method can meet the performance indicators of EVs in terms of power and energy for parameter matching. The result shows that optimized parameter matching is obtained by reducing the weight and cost.

Keywords: parameter matching method; battery-supercapacitor; electric vehicles; hybrid energy storage system

check for updates

Citation: Liu, F.; Wang, C.; Luo, Y. Parameter Matching Method of a Battery-Supercapacitor Hybrid Energy Storage System for Electric Vehicles. *World Electr. Veh. J.* **2021**, *12*, 253. https://doi.org/10.3390/wevj12040253

Academic Editor: Marie-Cécile Péra

Received: 15 September 2021
Accepted: 23 November 2021
Published: 1 December 2021

1. Introduction

Nowadays, the rapid growth of vehicles has led to energy shortages and environmental degradation [1]. Due to the advantages of low emissions and environmental friendliness, electric vehicles (EVs) have attracted extensive attention around the world [2]. As the main power sources, lithium-ion batteries are employed in EVs because of their merits of high energy density, low self-discharge rate, quick charging rate, and high nominal voltage. To efficiently achieve the operation requirements of EVs, a large number of individual lithium-ion battery cells are assembled in parallel series to form battery packs [3]. The high-rate charge and discharge of currents during driving dramatically reduce lithium-ion batteries' lifespan [4]. Lithium-ion batteries as the sole power source in vehicle power systems are well regarded as having apparent limitations. For example, the EVs cannot efficiently meet the needs of high-rate discharge currents in the circumstances of starting, acceleration, and hill climbing [5]. Moreover, the batteries suffer severe challenges in braking conditions. The surge current input reduces the vehicle power system's life and increases the battery's replacement cost [6].

In their present technological condition, the single power source of lithium-ion batteries has difficulties in meeting the requirements of both energy and power in EVs applications. Meanwhile, as power-based energy storage components, supercapacitors have the merits of high power density, broad working temperature, extended cycle life, and deep discharge ability [7–9]. Hybrid energy storage systems (HESS) in engineering applications consist of batteries and supercapacitors, which benefit from their respective advantages in terms of high energy density and high power density. The battery is the primary energy source that determines the driving ranges of EVs and supercapacitors are employed as an auxiliary power source to regulate peak power during starting, braking, accelerating, and hill climbing [10]. Supercapacitors can smooth the power of the battery and increase the flexibility of the HESS.

It is well known that the optimization of parameter matching between the battery pack and the supercapacitor pack can observably improve the efficiency of an HESS. In the past decades, many different parameter matching methods have been presented in the literature. Grün T, et al. [11] discussed the performances of a pure lithium-ion battery energy storage system and an HESS in the same volume and weight, and concluded that the HESS had a 22% increase in power density and a 15–30% reduction in load. In reference [12], the required power was split and the power at each moment was weighted to obtain the boundary conditions of parameter matching optimization. After optimizing, the weight of the battery pack was reduced by nearly 50%. The approach disregards adaptation to various driving cycles, and the results vary depending on the driving cycle. As a result, it is challenging to apply the strategy to EVs and obtain the desired outcomes. An equivalency factor of work condition prediction was introduced to the approach for the optimization of parameter matching in reference [13]; however, the accuracy of the prediction is not discussed, and the matching results are dynamically varied and slightly below the real demand. Yang et al. [14] used an NSGA-II-type genetic algorithm for parameter optimization and achieved some results. In particular, a cumulative penalty factor was added, considering the important indicator of capacity decay in service life. However, the adopted method was not selective in the type of supercapacitor monomer and battery monomer, meaning that the combined consideration of cost, lifetime, and price was highly constrained.

A novel battery-supercapacitor HESS parameter matching method for EVs is proposed in this paper, which combines the advantages of high energy density and high power density. This method is independent of the energy management strategy and has strong adaptability to the driving cycle. This method can meet the performance indicators of EVs in terms of power and energy for parameter matching. The optimized parameter matching results are obtained by reducing the weight and cost. The paper is organized as follows: Section 2 introduces the HESS topology categorization and the benefits of the chosen topology. Section 3 establishes a kinetic model, based on six typical operating conditions, and systematically analyzes its characteristic indexes. Section 4 analyzes the parameter matching methods and optimization results in detail. Finally, conclusions are given in Section 5.

2. HESS Topology

The battery-supercapacitor HESS mainly consists of a battery pack and a supercapacitor pack, a bidirectional DC/DC converter and a DC/AC inverter. In addition, it is divided into three topologies: semi-active, fully active, and passive parallel [15]. The three topologies are shown in Figure 1. In the semi-active topology, a bidirectional DC/DC converter is connected in series to the battery pack, and they connect with the supercapacitor pack in parallel [16]. In the fully active topology, the battery pack and the supercapacitor pack are connected in series with a bidirectional DC/DC converter, respectively. Then they are connected in parallel. Although the power can be accurately distributed, the energy of the supercapacitor pack is less, and the wide operating voltage will raise the energy loss. In the passive parallel topology, just the battery pack and supercapacitor pack are connected in parallel. Although this topology is simple, the power cannot be distributed, and the supercapacitor pack cannot fully demonstrate the advantages in power density [17]. Whether the supercapacitor pack is charged or discharged depends on the terminal voltage of the battery pack connected with the supercapacitor pack in parallel.

In this paper, the weight and cost are taken as the optimization objectives in the condition of reducing energy loss of the HESS, so the semi-active topology has been chosen. The supercapacitor pack is not affected by the battery pack voltage in this topology. Therefore, the role of supercapacitor pack can be fully utilized in this topology. The battery pack and the supercapacitor pack assume low and high power, respectively [18]. The supercapacitor pack undertakes transient high-power operation, and the battery pack avoids the effects of high-rate charging and discharging currents, to extend the HESS life of EVs [19]. Reference [20] discussed several complex topologies and their characteristics. The DC/DC converter that stabilizes the DC bus voltage function is impressive [21,22]. In the semi-active topology HESS, the DC/DC converter actively controls the rapid regulation of the battery pack voltage for precise power output [23]. In addition, it can stabilize the current and reduce the number of charges and discharges currents [20,24]. Where the supercapacitor pack absorbs, and its output power is passive, its rapid response depends on the fluctuation of the DC bus voltage [25]. In addition, the semi-active topology is easier to implement than the fully active topology control strategy [15,26].

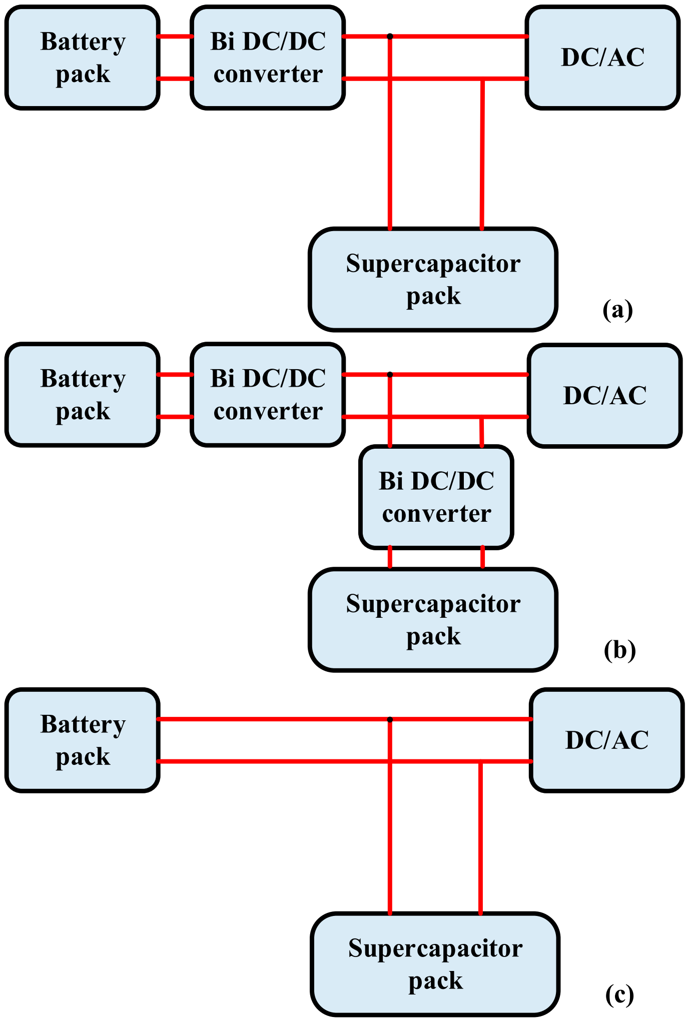

Figure 1. HESS topologies. (**a**) Semi-active; (**b**) fully active; (**c**) passive parallel.

3. Analysis of Six Typical Driving Cycles

The driving force and power requirement of the EVs are calculated as follows:

$$F_t = F_f + F_w + F_i + F_j = Mgf\cos\alpha + \frac{C_D A {v_a}^2}{21.15} + Mg\sin\alpha + \delta M\frac{dv_a}{dt} \tag{1}$$

$$P_{\text{req}} = \frac{1}{\eta} v_a \left[\frac{Mgf\cos\alpha}{3600} + \frac{C_D A {v_a}^2}{76140} + \frac{Mg\sin\alpha}{3600} + \frac{\delta M}{3600}\frac{dv_a}{dt}\right] \tag{2}$$

Formula (1) is the driving equation of the EVs. The driving force, the rolling resistance, air resistance, ramp resistance, and acceleration resistance are represented by F_t, F_f, F_w, F_i and F_j, respectively. Moreover, these resistances must be overcome to ensure the operation of EVs.

The driving power requirement is represented as Formula (2). Where P_{req} denotes the power demand, and the vehicle constant speed is set to v_a = 60 km/h. In addition, a vehicle model is selected in this paper, and the parameters and performance indicators are shown in Table 1.

Table 1. Parameters and performance indicators of the EV.

Parameter	Values
Curb weight M	1845 kg
Coefficient of air resistance C_D	0.36
Frontal area A	2.53 m^2
Rotating mass conversion factor δ	1.03
Acceleration of gravity g	9.8 m/s^2
Rolling resistance coefficient f	0.025
Transmission efficiency η	0.9
Driving ranges S	300 km
Maximum speed	130 km/h
Maximum grade α	25%
Rated busbar voltage U_m	360 V
Assisted acceleration time	15 s
0~50 km/h Acceleration time	≤10 s

Different driving cycles have their own specific characteristics of energy and power requirements. The characteristic parameters are mileage, driving time, average speed, maximum speed, and maximum acceleration, etc. The driving cycle can be divided into many cycle blocks, and the characteristic parameters of each block are correspondingly extracted. The energy demand and the maximum power demand are used to define the intensity factor of the cycle block [27]. In order to improve the fitness of the parameter matching method, six typical driving cycles, such as the highway road (HL07 and HWFET), urban road (UKBUS6 and NYCC), suburb road (INDIA_HWY_SAMPLE and WVUSUB), were selected in the system. The velocity–power curves of the six typical driving cycles are shown in Figure 2.

From Figure 2, it is obvious that the highway road, urban road, and suburb road have different performances. The highway road outputted successive medium–high power; the battery pack and the supercapacitor pack suffered from a severe challenge in optimizing the power distribution and maintaining stable output. The urban road had frequent processes of starting, accelerating, and braking, which require a more abundant supercapacitor pack. The speed of the suburban road changed more slowly than that of the urban road, and the overall energy and power requirements were between the urban road and the highway road.

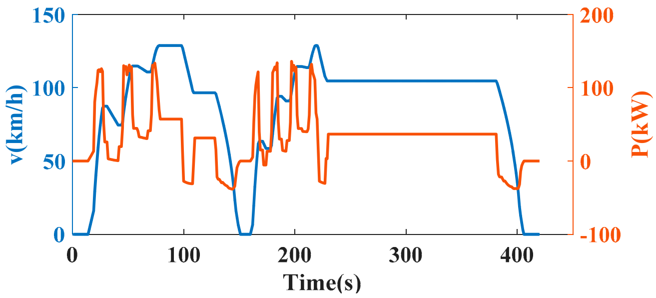

(**a**)

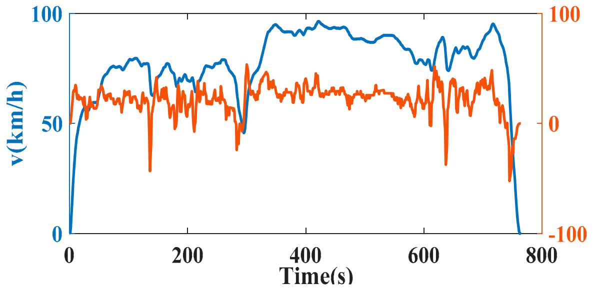

(**b**)

Figure 2. *Cont.*

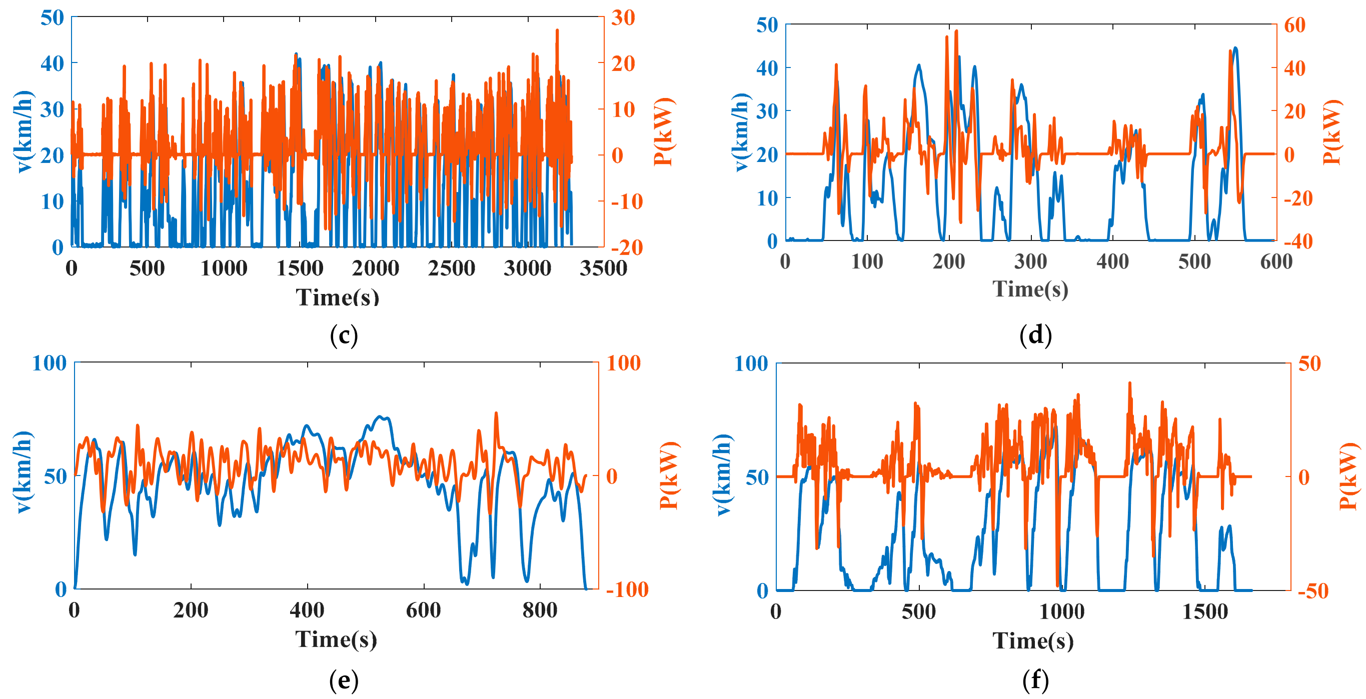

Figure 2. Velocity and power curves for six standard driving cycles. (**a**) HL07. (**b**) HWFET. (**c**) UKBUS6. (**d**) NYCC. (**e**) INDIA-HWY-SAMPLE. (**f**) WVUSUB.

However, different driving cycles have individual characteristics of maximum acceleration, positive peak power, positive average power, and negative peak power [28]. The power requirement characteristics for six typical driving cycles are shown in Table 2.

Table 2. Different driving cycles' power demand characteristics.

Driving Cycles/ Parameters	Maximum Acceleration (m/s^2)	Positive Peak Power (kW)	Positive Average Power (kW)	Negative Peak Power (kW)
HL07	3.576	135.822	45.816	−38.403
HWFET	1.431	53.606	24.790	−52.259
UKBUS6	1.313	27.093	4.871	−16.221
NYCC	2.682	56.956	9.564	−31.743
INDIA_HWY_SAMPLE	2.121	55.345	16.845	−33.525
WVUSUB	1.295	41.270	11.179	−48.049

From Table 2, it can be seen that highway roads, urban roads, and suburban roads chose long-duration and short-duration driving cycles, respectively. The maximum acceleration had no significant effect on different driving cycles. There was not much difference in maximum acceleration among HWFET in the highway driving cycle, UKBUS6 in the urban driving cycle, and WVUSUB in the suburban driving cycle. Moreover, the maximum acceleration (a_{max}) of HL07 can be as high as 3.576 m/s^2. There is a strong relationship between positive peak power and maximum acceleration. However, different road cycles reflected their unique characteristics. Compared with other driving cycles, the HL07 driving cycle had the largest positive peak power (P_{max}) of 135.822 kW and the largest positive average power (P_{avg}) of 45.816 kWh. The driving cycles of NYCC and UKBUS6 had the lowest positive average power. Because of the frequent acceleration followed by frequent braking in urban roads, the positive average power is always lower than that of other types of roads. The most widespread application of urban roads is necessary. The negative peak power appeared on highways and suburban roads before the end of the cycle, while urban roads performed with no discernible characteristics. The HWFET driving cycle had the largest negative peak power (P_{reg}) of -52.259 kWh. In summary, the six driving cycles are very rich and ensure the integrity of the HESS parameter matching.

4. HESS Parameter Matching Method and Optimization

The parameter matching method is very important in HESS application, and comprehensive analysis of battery and supercapacitor for EVs performance is necessary. In reality, the battery-supercapacitor HESS satisfies the requirements of capacity, power, output voltage, and other indicators to provide stable energy supply for EVs. In this paper, a power–energy-based parameter matching method is proposed to reasonably structure a HESS. The six typical driving cycles have specific power and energy requirements for the HEES, which can be described by the four constraint equations. The optimized designing scheme of HESS can achieve the power and energy requirements of EVs.

4.1. Energy Matching of Batteries

The energy match of the battery pack is mainly determined by the EV's driving ranges, which are set to 300 km in this paper.

$$S = \frac{E_{\text{req}} v_{\text{a}}}{P_{\text{req}}} \tag{3}$$

$$E_{\text{req}} = E_{\text{Bat}} \times n_{DOD} \tag{4}$$

$$1000 E_{\text{Bat}} = C_{\text{Bat-cell}} U_{\text{Bat-cell}} N_{\text{Bat-s}} N_{\text{Bat-p}} \tag{5}$$

$$N_{\text{Bat-s}} = \frac{U_{\text{m}}}{U_{\text{Bat-cell}}} \tag{6}$$

In Formula (3), S is the driving range [29]. E_{req} and P_{req}, respectively, denote energy demand and power demand. v_{a} is the given ideal speed. The depth of discharge is n_{DOD} =0.8, and the battery energy demand E_{Bat} is 86.5017 kWh. $N_{\text{Bat-p}}$ is the number of batteries in parallel, $C_{\text{Bat-cell}}$ is the battery cell capacity, and Formula (5) is the first constraint. In Formula (6), U_{m} is the bus rated voltage, $U_{\text{Bat-cell}}$ is the battery cell voltage, $N_{\text{Bat-s}}$ is the number of batteries in series [6,29].

4.2. Energy Matching of Supercapacitors

The highest energy requirements often occur in the conditions of starting, acceleration and braking. Therefore, the supercapacitors are assistantly employed to satisfy the energy demand. The starting energy, acceleration energy, and braking energy are caculated as follows:

$$E_{\text{star}} = \int_0^t F v(t) dt \tag{7}$$

$$E_{\text{ass}} = \frac{1}{3600} \int_0^t (P_{\text{ass}}(t) - P_{\text{avg}}(t)) dt \tag{8}$$

$$E_{\text{reg}} = \frac{1}{3600} \left(\int_0^t P_{\text{reg}}(t) dt \right) \tag{9}$$

$$E_{\text{sc}} \geq \max(E_{\text{star}}, E_{\text{ass}}, E_{\text{reg}}) \tag{10}$$

The supercapacitor is used to absorb and output transient high-rate current due to its excellent properties of rapid charge and discharge. From Table 2, the maximum acceleration (a_{max}) is 3.576 m/s^2, out of all driving cycles. In Formula (7), E_{star}= 0.0494 kWh represents the starting energy of the EV when accelerating to 50 km/h at maximum acceleration. In Formula (8), E_{ass} denotes the acceleration energy of 0.3750 kWh. P_{avg} is the maximum positive average power of 45.816 kW, P_{ass} is the maximum positive peak power of 135.822 kW, and the assisted acceleration time t is 15 s [30]. In Formula (9), E_{reg} represents energy recovered from braking. P_{reg} denotes the maximum negative peak power of −52.259 kW. The braking time is set as 2 s in this paper, and the braking energy is 0.0290 kWh.

$$E_{sc} = \frac{1}{3600}\frac{1}{2}N_{sc-s}N_{sc-s}C_{sc}\left(U^2_{sc\ max} - U^2_{sc\ min}\right) \tag{11}$$

The capacity of the supercapacitor conforms to Ohm's law between the pack and the cell [31]. In Formula (11), N_{sc-s} is the number of supercapacitors in series, N_{sc-p} is the number of supercapacitors in parallel, C_{sc} is the supercapacitor cell capacity, $U_{sc\ max}$ is the upper cut-off voltage of supercapacitors equal to 2.7 V, and $U_{sc\ min}$ is the lower cut-off voltage of supercapacitors equal to 1.35 V.

$$C_{sc} \geq \frac{3600 \times 2 \times 1000 \times \max(E_{star}, E_{ass}, E_{reg})}{N_{sc-s}N_{sc-p}(U^2_{sc\ max} - U^2_{sc\ min})} \tag{12}$$

Substitute Formulas (7)–(10) into Formula (11) to obtain Formula (12), which is the second constraint.

4.3. Power Matching Method

The battery and supercapacitor satisfied the maximum power requirements in the HESS. Where the battery pack supports the maximum average power, the supercapacitor pack supports the residual power.

$$P_{bat} + P_{sc} \geq P_{max} \tag{13}$$

$$P_{bat} = P_{avg-max} \tag{14}$$

$$P_{sc} = N_{sc-s}N_{sc-p}m\rho_{sc} \tag{15}$$

$$N_{sc-s}N_{sc-p}m\rho_{sc} \geq P_{max} - P_{avg-max} \tag{16}$$

$$kC_{bat}U_{bat} \geq P_{avg-max} \tag{17}$$

where m represents the weight of the supercapacitor cell. The parameters of the battery and the supercapacitor are summarized in Section 4.4. ρ_{sc} is power density of the supercapacitor, k is the current rate, and $P_{avg-max}$ is the maximum value of the average power in the six typical driving cycles. This can effectively avoid the high charge and discharge rate of the battery. Formulas (16) and (17) are the third and fourth constraints, respectively. Here, $kC_{bat} = 2C_{bat}$—the unit is ampere. It is generally believed that the working current exceeding 2C will reduce the cycle life of the battery [10].

4.4. Optimization Results

The purpose of HESS parameter matching is to optimize the combination of battery and supercapacitor to ensure the power performance of EVs. The HESS parameter matching method consists of the following three steps: First, a kinetic equation is developed based on the identified vehicle model and six typical driving cycles are analyzed in detail for power demand and criticality. Second, the energy and power requirements of the battery and supercapacitor are systematically calculated under the relevant constraints. Third, the parameters of the composite power supply are optimally matched, based on the consideration of performance parameters, cost, and weight. The following is the optimized selection, based on the four constraints mentioned above.

Table 3 shows the cell capacity selection range of batteries and supercapacitors under different parallel scales, which are obtained by Formulas (5) and (12).

Formula (5) can be used to obtain the requirements of the number of parallel connections for batteries of different capacities in Table 4, where ρ_{bat} represents the battery unit energy density and W_{bat} denotes battery unit energy price.

Table 3. The capacity ranges of cell under different parallels.

N_{Bat-p}	$C_{Bat-cell}$ (Ah)	N_{sc-p}	C_{sc} (F)
1	$\geq$233.790	1	$\geq$3658.198
2	$\geq$116.900	2	$\geq$1829.099
3	$\geq$77.930	3	$\geq$1219.399
4	$\geq$58.450	4	$\geq$914.549
5	$\geq$46.760	5	$\geq$731.639
6	$\geq$38.965	6	$\geq$609.699
7	$\geq$33.400	7	$\geq$522.599
8	$\geq$29.220	8	$\geq$457.275
9	$\geq$25.970	9	$\geq$406.466
10	$\geq$23.380	10	$\geq$365.820

Table 4. The parallel range under different batteries' capacities.

$C_{Bat-cell}$ (Ah)	N_{Bat-p}	m (kg)	ρ_{bat} (Wh/kg)	W_{bat} ($/Wh)
25	$\geq$9.352	0.585	170	0.430
35	$\geq$6.680	1.080	135	0.430
60	$\geq$3.900	1.850	130	0.430
100	$\geq$2.338	3.050	115	0.430

Formulas (12) and (16) can be used to obtain the requirements for the number of parallel connections of supercapacitors of different capacities in Table 5, where ρ_{sc} is the supercapacitor power density, and W_{sc} is the energy price of the supercapacitor.

Table 5. The parallel range under different supercapacitors' capacities.

C_{sc} (F)	ρ_{Esc} (Wh/kg)	m (kg)	ρ_{sc} (W/kg)	W_{sc} ($/Wh)	N_{sc-p}
650	3.29	0.20	5400	11.55	$\geq$6.173
1200	4.05	0.30	5000	11.55	$\geq$4.444
1500	4.75	0.32	5800	11.55	$\geq$3.592
2000	5.06	0.40	6200	11.55	$\geq$2.688
3000	5.52	0.55	5400	11.55	$\geq$2.245

In summary, the above four Formulas—(5), (12), (16) and (17)—are the constraints of the parameter matching method. In view of these four constraints, it is possible to achieve two-way optimal selection, by selecting the serial–parallel scale of the known single element specifications and the preset scale of selecting the specifications of the single element. The method in this paper is more comprehensive in terms of weight and cost, as well as more adaptable and practical in HESS. However, because each model has its own price, capacity, and weight, the greatest impact for the specific optional battery model and matching parameters must be determined first. In this paper, NMC lithium-ion batteries with capacities of 25 Ah, 35 Ah, 60 Ah, and 100 Ah were selected. Simultaneously, the chosen supercapacitors were made by Maxwell and had rated capacities of 650 F, 1500 F, 2000 F, and 3000 F, respectively. Tables 6 and 7 show the minimum weight and the lowest cost after matching the parameters of different capacity batteries and different capacity supercapacitors, respectively.

Table 6. Batteries of different capacities matching results.

$C_{Bat-cell}$ (Ah)	25	35	60	100
minN_{Bat-p}	10	7	4	3
min weight (kg)	585	756	740	915
min cost (k$)	42.763	43.886	41.366	45.247

Table 7. Supercapacitors of different capacities matching results.

C_{sc} (F)	650	1200	1500	2000	3000
minN_{sc-p}	7	5	4	3	3
min weight (kg)	189.0	202.5	172.8	162.0	222.8
min cost (k$)	7.181	9.472	9.480	9.468	14.201

Furthermore, the goal function is as follows.

$$J(x) = \alpha M_1 + \beta M_2 + \eta C_1 + \lambda C_2 \tag{18}$$

$$M_1 = N_{\mathrm{Bat-s}} N_{\mathrm{Bat-p}} m \tag{19}$$

$$M_2 = N_{\mathrm{sc-s}} N_{\mathrm{sc-p}} m \tag{20}$$

$$C_1 = N_{\mathrm{Bat-s}} N_{\mathrm{Bat-p}} m \rho_{\mathrm{bat}} \tag{21}$$

$$C_2 = N_{\mathrm{sc-s}} N_{\mathrm{sc-p}} m \rho_{Esc} \tag{22}$$

where M_1 and M_2 represent the battery pack and the supercapacitor pack weight, respectively. C_1 and C_2 represent battery and supercapacitor cost, respectively. α and β are the weight coefficients for battery pack weight and supercapacitor pack weight, respectively. η and λ represent the weight coefficients for battery pack cost and supercapacitor pack cost, respectively. Its range is from 0 to 1. In addition, the weight coefficients must satisfy $\alpha + \beta = 1$ and $\eta + \lambda = 1$. If $\alpha = \beta = \eta = \lambda$= 0.5, cost ($C_1$,$C_2$) and weight ($M_1$,$M_2$) are optimization targets with equal weights. If the cost is the only optimization objective, point A is the optimization result, with $C_1 + C_2$= 48.547 k$, $M_1 + M_2$ = 929.0 kg, N_{Bat-p}= 4, and N_{sc-p}= 7. The selected battery and supercapacitor have capacities of 60 Ah and 650 F, respectively. If M is the only optimization objective, then point C is the optimization result, with $C_1 + C_2$ = 52.231 k$, $M_1 + M_2$ = 747.0 kg, N_{Bat-p}= 10, and N_{sc-p}= 3. The selected battery and supercapacitor have capacities of 25 Ah and 2000 F, respectively. Considering the difference in weight and cost between the supercapacitor and the battery. Supercapacitors have a longer lifespan, so β is greater than α and λ is greater than η.

In this paper, point B is the selected result, with $C_1 + C_2$ = 52.245 k$, $M_1 + M_2$ = 757.8 kg, N_{Bat-p} = 10, N_{sc-p} = 4, battery capacity $C_{Bat-cell}$ = 25 Ah, and supercapacitor capacity C_{sc} = 1500 F. Figure 3 shows the HESS parameter optimization results.

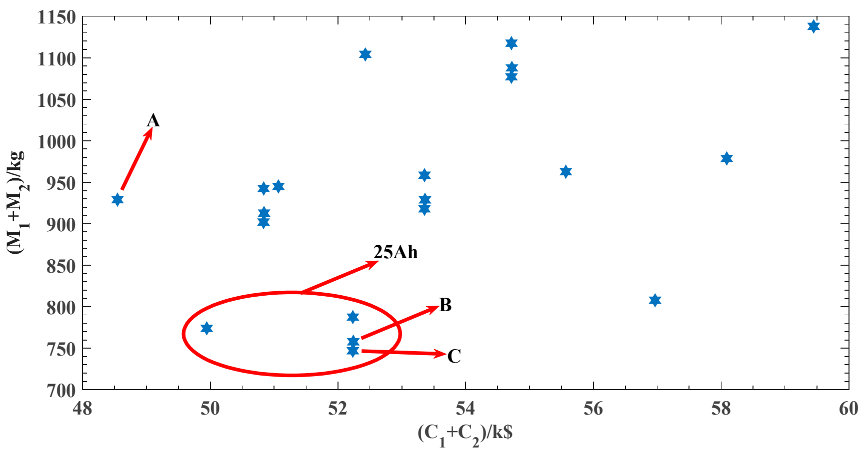

Figure 3. The HESS parameter optimization results.

5. Conclusions

A comprehensive analysis of the HESS parameter matching method for EV is presented in this work. Parameter matching is a step in the energy management system (EMS) process, and accurate parameter matching offers EMS benefits and potential. First, a superior semi-active topology was selected to establish the HESS. Based on the major characteristics and key indications of the EV, a detailed study of the steady-state energy and transient power requirements of the normal driving cycle were addressed. The computation of the HESS threshold is investigated in order to optimize the HESS structure based on a cost–weight balance. In addition, the effect of the series and parallel connections between the battery and supercapacitor on energy and capacity is investigated. The parameter matching method proposed in this paper can be further applied in the EV field.

Author Contributions: Conceptualization, F.L., C.W. and Y.L.; methodology, F.L.; software, F.L.; validation, F.L. and C.W.; formal analysis, F.L. and C.W.; investigation, C.W.; resources, C.W.; data curation, F.L.; writing—original draft preparation, F.L.; writing—review and editing, F.L. and C.W.; visualization, F.L. and C.W.; supervision, C.W. and Y.L.; project administration, C.W.; funding acquisition, C.W. All authors have read and agreed to the published version of the manuscript.

Funding: This research was funded by the National Natural Science Foundation of China (Grant No. 51907136), Zigong Key Science and Technology Project (Grant No. 2019YYJC14), and Talent Introduction Project of Sichuan University of Science & Engineering (Grant No. 2019RC15). The systemic experiments were performed at the Advanced Energy Storage and Application (AESA) Group, Beijing Institute of Technology.

Conflicts of Interest: The authors declare no conflict of interest.

References

1. Yan, Z.; Zhang, Y.; Liang, R.; Jin, W. An allocative method of hybrid electrical and thermal energy storage capacity for load shifting based on seasonal difference in district energy planning. *Energy* **2020**, *207*, 118139. [CrossRef]
2. Chen, Z.; Guo, N.; Shen, J.; Xiao, R.; Dong, P. A hierarchical energy management strategy for power-split plug-in hybrid electric vehicles considering velocity prediction. *IEEE Access* **2018**, *6*, 33261–33274. [CrossRef]
3. Xiong, R.; Sun, F.C.; Gong, X.Z.; Gao, C.C. A data-driven based adaptive state of charge estimator of lithium-ion polymer battery used in electric vehicles. *Appl. Energy* **2014**, *113*, 1421–1433. [CrossRef]
4. Hannan, M.A.; Lipu, M.S.H.; Ker, P.J.; Begum, R.A.; Agelidis, V.G.; Blaabjerg, F. Power electronics contribution to renewable energy conversion addressing emission reduction: Applications, issues, and recommendations. *Appl. Energy* **2019**, *251*, 113404. [CrossRef]
5. Randive, V.; Subramanian, S.C.; Thondiyath, A. Design and Analysis of a Hybrid Electric Powertrain for Military Tracked Vehicles. *Energy* **2021**, *229*, 120768. [CrossRef]
6. Song, Z.; Li, J.; Hou, J.; Hofmann, H.; Ouyang, M.; Du, J. The battery-supercapacitor hybrid energy storage system in electric vehicle applications: A case study. *Energy* **2018**, *154*, 433–441. [CrossRef]
7. Zhang, S.; Xiong, R.; Cao, J.Y. Battery durability and longevity based power management for plug-in hybrid electric vehicle with hybrid energy storage system. *Appl. Energy* **2016**, *179*, 316–328. [CrossRef]
8. Liu, K.; Yu, C.; Guo, W.; Lin, N.; Yu, J.; Xie, Y.; Wang, Z.; Ren, Y.; Qiu, J. Recent research advances of self-discharge in supercapacitors: Mechanisms and suppressing strategies. *J. Energy Chem.* **2021**, *58*, 94–109. [CrossRef]
9. Gomez-Gonzalez, M.; Hernández, J.C.; Vidal, P.G.; Jurado, F. Novel optimization algorithm for the power and energy management and component sizing applied to hybrid storage-based photovoltaic household-prosumers for the provision of complementarity services. *J. Power Sources* **2021**, *482*, 228918. [CrossRef]
10. Wang, C.; Huang, B.; Xu, W. An integrated energy management strategy with parameter match method for plug-in hybrid electric vehicles. *IEEE Access* **2018**, *6*, 62204–62214. [CrossRef]
11. Grün, T.; Smith, A.; Ehrenberg, H.; Doppelbauer, M. Passive Hybrid Storage Systems: Influence of circuit and system design on performance and lifetime. *Energy Procedia* **2018**, *155*, 336–349. [CrossRef]
12. Catenaro, E.; Rizzo, D.M.; Onori, S. Framework for energy storage selection to design the next generation of electrified military vehicles. *Energy* **2021**, *231*, 120695. [CrossRef]
13. Zeng, T.; Zhang, C.; Zhang, Y.; Deng, C.; Hao, D.; Zhu, Z.; Ran, H.; Cao, D. Optimization-oriented adaptive equivalent consumption minimization strategy based on short-term demand power prediction for fuel cell hybrid vehicle. *Energy* **2021**, *227*, 120305. [CrossRef]
14. Yang, J.B.; Xu, X.H.; Peng, Y.Q. Optimal Parameter Matching of Hybrid Energy Storage System Based on NSGA-II Algorithm for Energy Storage Type Tram. *Chin. J. Mech. Eng.* **2020**, *56*, 181–189.
15. Kouchachvili, L.; Yaïci, W.; Entchev, E. Hybrid battery/supercapacitor energy storage system for the electric vehicles. *J. Power Sources* **2018**, *374*, 237–248. [CrossRef]
16. Khasim, S.R.; Dhanamjayulu, C. Selection parameters and synthesis of multi-input converters for electric vehicles: An overview. *Renew. Sustain. Energy Rev.* **2021**, *141*, 110804. [CrossRef]

17. Wieczorek, M.; Lewandowski, M. A mathematical representation of an energy management strategy for hybrid energy storage system in electric vehicle and real time optimization using a genetic algorithm. *Appl. Energy* **2017**, *192*, 222–233. [CrossRef]
18. Li, Y.; Huang, X.; Liu, D.; Wang, M.; Xu, J. Hybrid energy storage system and energy distribution strategy for four-wheel independent-drive electric vehicles. *J. Clean. Prod.* **2019**, *220*, 756–770. [CrossRef]
19. Wang, C.; Xiong, R.; He, H.W.; Ding, X.F.; Shen, W.X. Efficiency analysis of a bidirectional DC/DC converter in a hybrid energy storage system for plug-in hybrid electric vehicles. *Appl. Energy* **2016**, *183*, 612–622. [CrossRef]
20. Wang, Y.; Sun, Z.; Chen, Z. Development of energy management system based on a rule-based power distribution strategy for hybrid power sources. *Energy* **2019**, *175*, 1055–1066. [CrossRef]
21. Xiong, R.; Cao, J.; Yu, Q. Reinforcement learning-based real-time power management for hybrid energy storage system in the plug-in hybrid electric vehicle. *Appl. Energy* **2018**, *211*, 538–548. [CrossRef]
22. Chen, H.; Zhang, Z.; Guan, C.; Gao, H. Optimization of sizing and frequency control in battery/supercapacitor hybrid energy storage system for fuel cell ship. *Energy* **2020**, *197*, 117285. [CrossRef]
23. Xiong, R.; Chen, H.; Wang, C.; Sun, F. Towards a smarter hybrid energy storage system based on battery and ultracapacitor—A critical review on topology and energy management. *J. Clean. Prod.* **2018**, *202*, 1228–1240. [CrossRef]
24. Zhou, F.; Xiao, F.; Chang, C.; Shao, Y.; Song, C. Adaptive model predictive control-based energy management for semi-active hybrid energy storage systems on electric vehicles. *Energies* **2017**, *10*, 1063. [CrossRef]
25. Sarwar, W.; Engstrom, T.; Marinescu, M.; Green, N.; Taylor, N.; Offer, G. Experimental analysis of Hybridised Energy Storage Systems for automotive applications. *J. Power Sources* **2016**, *324*, 388–401. [CrossRef]
26. Wang, Y.; Wang, L.; Li, M.; Chen, Z. A review of key issues for control and management in battery and ultra-capacitor hybrid energy storage systems. *eTransportation* **2020**, *4*, 100064. [CrossRef]
27. Song, Z.; Hou, J.; Xu, S.; Ouyang, M.; Li, J. The influence of driving cycle characteristics on the integrated optimization of hybrid energy storage system for electric city buses. *Energy* **2017**, *135*, 91–100. [CrossRef]
28. Wu, Y.; Li, C.; Tian, Z.; Sun, J. Solar-driven integrated energy systems: State of the art and challenges. *J. Power Sources* **2020**, *478*, 228762. [CrossRef]
29. Hu, J.J.; Xiao, J.; Yan, J.J. Control strategy and parameter optimization of hybrid energy storage device for electric vehicles. *J. Chongqing Univ.* **2016**, *39*, 1–11.
30. Liu, C.; Wang, Y.; Wang, L.; Chen, Z. Load-adaptive real-time energy management strategy for battery/ultracapacitor hybrid energy storage system using dynamic programming optimization. *J. Power Sources* **2019**, *438*, 227024. [CrossRef]
31. Song, Z.; Hofmann, H.; Li, J.; Han, X.; Ouyang, M. Optimization for a hybrid energy storage system in electric vehicles using dynamic programing approach. *Appl. Energy* **2015**, *139*, 151–162. [CrossRef]